Biomedicine & Pharmacotherapy 180 (2024) 117552

Contents lists available at ScienceDirect

Biomedicine & Pharmacotherapy

journal homepage: www.elsevier.com/locate/biopha

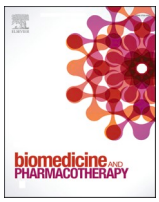

Antimigratory effects of a new NF-κB inhibitor, (S)-b-salicyloylamino-a-exo-methylene-γ-butyrolactone, in 2D and 3D breast cancer models

Paola Poma [a,*], Salvatrice Rigogliuso [a], Manuela Labbozzetta [a], Francesco Carfì Pavia [b], Camilla Carbone [b], Jun Ma [c], Alessandra Cusimano [a], Monica Notarbartolo [a]

[a] Department of Biological, Chemical, and Pharmaceutical Sciences and Technologies (STEBICEF), University of Palermo, Palermo, Italy
[b] Department of Engineering, University of Palermo, Palermo, Italy
[c] Department of Research and Development, Shenzhen Wanhe Pharmaceutical Co., Ltd., Shenzhen, China

ARTICLE INFO

[†] Dedicated to the memory of Professor Kazuo Umezawa

Keywords:
Breast cancer
SEMBL
NF-κB
Invasive ability
Vimentin
PLLA scaffolds

ABSTRACT

One of the pharmacological approaches to neoplastic disease aims to target the metastatic capacity of tumor cells to reduce their aggressive behavior. In this study, we analyzed the antimigratory capacity of the compound SEMBL, (S)-β-salicyloylamino-a-exo-methylene-γ-butyrolactone, a new analog of (-)-Dehydroxymethylepoxyquinomicin ((-)-DHMEQ), in three different breast cancer cell lines: MCF-7, MCF-7R and MDA-MB-231. This molecule is characterized by intense antiproliferative activity, evaluated by MTS assay, showing greater potency than DHMEQ. SEMBL was able to inhibit nuclear factor κappa B (NF-κB) activation observed through TransAM™ assay, while cell invasion and wound healing assays revealed a strong reduction in invasive capacity mediated by metalloproteinase 2 (MMP-2) and Vimentin decrease. These results, obtained *in vitro*, were corroborated on 3D systems made up of Poly-L-Lactic Acid (PLLA) scaffolds. In summary, SEMBL exerts interesting anti-tumor activities in preclinical breast cancer models and therefore it could be a promising new molecule to be studied also in other types of neoplastic disease.

1. Introduction

Breast cancer is today the leading cause of cancer death among women. Even if the therapeutic options have significantly increased together with screening and prevention programs that anticipate diagnoses, the incidence remains very high [1]. The World Health Organization (WHO) published a new Global Breast Cancer Initiative Framework guidance to meet the goals of saving 2.5 million lives from breast cancer by 2040. The very high molecular heterogeneity of breast cancer makes it difficult to provide a hormonal or biological therapy suitable for all subtypes (The Cancer Genome Atlas Network, 2012). Unfortunately, BC is characterized by extensive metastatic capacity which is often the cause of treatment failure and a poor outcome. The epithelial-to-mesenchymal transition (EMT) is considered one of the major mechanisms involved in solid tumor metastasis, but not the only one. The use of matrix metalloprotease inhibitors and serine endopeptidases, including Seprase and Dipeptidyl peptidase-4 inhibitors (DPP-4), known to be involved in remodeling of the extracellular matrix (ECM) during angiogenesis, is useful for inhibiting mesenchymal migration [2]. However, it does not affect the multiple processes that determine invasiveness, such as the mesenchymal-ameboid transition (MAT) or the opposite process, the ameboid-mesenchymal transition (AMT). Brabek et al. have coined the term “migrastatic” to define antimetastatic compounds able to block all invasiveness and metastasis processes [3].

(-)-Dehydroxymethylepoxyquinomicin ((-)-DHMEQ) is an NF-κB inhibitor that was shown to suppress various disease models *in vivo* [4,5]. In the present research, we evaluated the antimigratory ability of (S)-β-salicyloylamino-a-exo-methylene-γ-butyrolactone (SEMBL), a new analog of DHMEQ [6]. SEMBL possesses exo-ene instead of epoxide, and it is a stable analog of DHMEQ acting with the same mechanism.

NF-κB is a transcription factor that promotes the expression of many inflammatory cytokines, adhesion molecules, anti-apoptosis proteins and metastasis-promoting proteins such as VEGFs and matrix metalloproteinases (MMPs). However, its excessive activation often induces inflammation and contributes to cancer progression. There is growing

* Corresponding author.
E-mail address: paola.poma@unipa.it (P. Poma).

https://doi.org/10.1016/j.biopha.2024.117552
Received 12 August 2024; Received in revised form 30 September 2024; Accepted 8 October 2024
0753-3322/© 2024 The Authors. Published by Elsevier Masson SAS. This is an open access article under the CC BY license (http://creativecommons.org/licenses/by/4.0/).

evidence that aberrant activation of nuclear factor NF-κB signaling is a frequent feature of breast cancer and is associated with its EMT and a high propensity for early metastasis [7] thus, NF-κB is considered to be an attractive target for drug discovery. For this purpose, we used three BC cell lines with different histotype and molecular characteristics: MCF-7 (human adenocarcinoma cells with ER^+, PR^+, $HER2^+$), its multi-drug resistant variant MCF-7R and MDA-MB-231 (human adenocarcinoma triple negative breast cancer cells).

Although traditional two-dimensional (2D) cell cultures are the gold standard in cancer research, they often fail to mimic the complexity of the tumor *in vivo* microenvironment, decelerating the development of effective therapeutic strategies [8]. The cell-matrix interactions can influence processes such as cell proliferation, migration, and the formation of multicellular tumor spheres, thereby accurately reflecting tumor behavior. In this paper Poly-L-Lactic Acid (PLLA) scaffolds were used as an *in vitro* 3D model; these can be a useful tool in recreating the ideal microenvironment for the regulatory mechanisms between tumor and stromal component. For these reasons, the same test carried out in 2D, on the three cell lines, were conducted in parallel on the 3D support.

2. Materials and methods

2.1. Materials

(S)-b-salicyloylamino-a-exo-methylene-γ-butyrolactone (SEMBL Lot No 20170602) was synthesized by Prof. Kazuo Umezawa according to the method described before [6]. The purity of the compound used was 95.79 % (Supplementary materials) determined as described below.

2.2. High performance liquid chromatography

The HPLC of the SEMBL compound (Lot No 20170602) was carried out according to the following procedures:

Diluent: Pipet 1 mL of phosphoric acid to a 1000 mL volumetric flask, dilute with dimethyl sulfoxide to volume, and mix. *Blank:* Diluent. *Sample solution:* Accurately weigh a suitable quantity of the product, dissolve with diluent and dilute to obtain a solution having a concentration of about 1 mg/mL.

Chromatographic system: The liquid chromatograph is equipped with an analytical column maintained at 35 ℃ containing packing C18 (such as Welch AQ C18 column, 4.6*250 mm, 5 μm, or equivalent). The mobile phase is acetonitrile-0.05 % phosphoric acid (30:70, v/v) (0.05 % phosphoric acid: pipet 0.5 mL of phosphoric acid to a 1000 mL volumetric flask, dilute with water to volume, and mix), and the flow rate is about 1.0 mL per minute. The detector wavelength number is 238 nm, the injection volume is 10 μl, and the run time is 40 minutes. *Procedure:* Separately inject equal portions, accurately measured, of the sample solution and the Blank into the chromatograph and record the chromatograms. Calculated by peak area normalization method.

Instrument: DIONEX UliMate3000 High performance liquid chromatograph. *Chromatographic column*: Welch ultimate AQ-C18 4.6*250 mm, 5 μm. Phosphoric acid: Tianjin Kemiou Chemical Reagent Co., Ltd., HPLC grade, lot no.: 20230619. Dimethyl sulfoxide: Honeywell, HPLC grade, lot no.: DQ408. Acetonitrile: Fisher chemical, HPLC grade, lot no.: F22MB7205.

2.3. Cell lines and culture conditions

The human breast cancer cell lines MCF-7 and MDA-MB-231 were obtained from ATCC (respectively HTB-22™ and HTB-26™, Rockville, MD, USA). The multi drug resistance (MDR) cell line MCF-7R was established treating the wild-type cells with gradually increasing concentrations of doxorubicin. The IC_{50} value of doxorubicin in MCF-7R is approximately 75 times higher than the original IC_{50}. Unlike MCF-7, MCF-7R lacks ERα expression, is estrogen-insensitive and overexpresses P-glycoprotein, as demonstrated in our laboratory using mRNA and protein expression analyses and cell viability assays examining the response of cells to diethylstilbestrol, tamoxifen and some molecules with an antiblastic action. MCF-7R cell line, in addition is characterized by a constitutive activation of the NF-κB pathway, and by the overexpression of some targets of this transcription factor such as Inhibitor of Apoptosis Proteins (IAPs) which determine its resistance to drug-induced cell death. Additionally, a triple-negative breast cancer (TNBC) cell line, MDA-MB-231, characterized by the absence of estrogen receptor (ER-), progesterone receptor (PR-) and Human Epidermal Growth Factor Receptor 2 (HER2) was also analyzed. The triple-negative carcinoma is associated with epithelial-mesenchymal transition (EMT) and a high propensity towards early metastases. Prof. Giulio Ghersi (STEBICEF Department, University of Palermo, Italy) kindly provided us with the non-tumorigenic cell line 1–7HB2 (ECACC 10081201—Cancer Research Technology, London, UK). Breast cancer cell lines were cultured in Dulbecco's Modified Eagle Medium (DMEM) (HyClone Europe Ltd, Cramlington, UK), while 1–7HB2 was cultured in DMEM low glucose supplemented with hydrocortisone (5 μg/mL) and insulin (10 μg/mL). All media were further supplemented with 10 % heat-inactivated fetal calf serum, 2 mM L-glutamine, 100 units/mL penicillin and 100 μg/mL streptomycin (all reagents were from HyClone Europe). All cell lines were cultured in a humidified atmosphere of 5 % CO_2 at 37 °C. Cells with a narrow range of passage numbers were used for all experiments. The cultures, maintained as monolayers in complete medium, were routinely tested for Mycoplasma infection and then, when cells reach the 80 %-90 % confluence were enzymatically recovered with trypsin and used in the experiments described below.

2.4. Scaffold preparation

PLLA scaffold were prepare according to a previous work of the authors [9]. Briefly, the polymer (Resomer^{TN} L 209 S) was dissolved into 1,4 dioxane (Merck KGaA, Darmstadt, Germany) with a concentration of 4 % (wt/wt) at a temperature of 120 °C. Then distilled water was added until reaching a dioxane to water weight ratio of 87/13. 5 mL of the solution, kept at 60 °C, were poured into a High-Density Poly-Ethylene (HDPE) cylindrical sample holder (innerdiameter 17.6 mm and 35.7 mm height). The sample holder was then immersed into a thermostatic water bath at the temperature of 20 °C (demixing temperature), for 15 minutes (demixing time). Finally, the system was suddenly quenched by pool immersion in an ethyl alcohol bath at a temperature of −20 °C for at least 10 min to stop the process of demixing and freeze the as-obtained structure. The as-obtained samples were subjected to washing in deionised water and drying at 35 °C under vacuum, to completely remove any remaining solvent trace. For the cell seeding assay, cylindrical scaffolds were first transversally cut onto a 2 mm disk and then misshapen into 3,5 mm-diameter and 2 mm-height cylinders using a biopsy punch.

2.5. Cell proliferation assay in 2D and 3D conditions

Cell lines were seeded at 5×10^3 cells/well in 96-well plates and incubated overnight at 37 °C. At time 0, the medium was replaced with fresh complete medium supplemented with SEMBL at the indicated concentrations. Respectively after 24, 48 and 72 h of treatment, 16 μl of a commercial solution (Promega Corporation Madison, WI, USA) containing 3- (4,5-dimethylthiazol-2-yl) −5- (3-carboxymethoxyphenyl) -2- (4-sulfophenyl) -2H-tetrazolium (MTS) and phenazine ethosulfate, was added. The plates were incubated in a humidified atmosphere at 37 °C in 5 % CO_2 for 2 h, and the bioreduction of the MTS dye was evaluated by measuring the absorbance of each well at 490 nm using a microplate reader (iMark Microplate Reader; BioRad Laboratories, Inc., Hercules,CA, USA). Cell growth inhibition was expressed as a percentage (mean ± SE) of absorbance compared to control cells.

For the 3D assays evaluated by MTS assay according to the manufacturer's instructions, growth tests were carried out on PLLA scaffolds.

The scaffolds were sterilized in 70 % ethanol under vacuum for 8 hours, washed in Phosphate Buffered Saline (PBS), and soaked in Dulbecco's modified Eagle's-high glucose medium (DMEM, Sigma Aldrich, Italy) to increase their hydrophilicity. Then, a cell suspension of 4×10^4 cells/mL was seeded into each scaffold and after 1 hour, the multiwell plate containing the scaffolds was filled with complete medium. A time of 5 days was considered optimal and established as time 0 for all subsequent 3D experiments. For the evaluation of cell viability, the samples were incubated in 96-well plate in a complete culture medium supplemented with SEMBL at the indicated concentrations. After 72 h of incubation, 16 µl of MTS solution was added and the absorbance of the supernatant was measured with a microplate reader. A cell-free scaffold was used as a blank. All tests were performed in triplicate.

2.6. Cell death and cell cycle analysis

To determine cell death, MCF-7, MCF7-R and MDA-MB-231 cells (1×10^5) were treated for 24, 48 and 72 h with SEMBL at the respective IC_{50} values. The Annexin V-Cy3/SYTOX Green (BioVision, CA, USA) apoptosis kit was used, which is able to distinguish apoptosis from necrosis by staining with both Annexin V-Cy3 and SYTOX Green. Following the incubations, cells were collected and washed twice with ice-cold PBS and then resuspended in 500 µL of 1X binding buffer. 5 µL of Annexin V-Cy3 and 1 µL of SYTOX Green were added. Samples were incubated at room temperature for 10–20 min in the dark and subsequently quantified by flow cytometry. The data were analyzed by Flow Jo Software v10.

To determine cell-cycle distribution, the three cell lines were treated for 72 h with SEMBL at the respective IC_{50} values. After treatment, cells were collected and washed with ice-cold PBS and then resuspended at 1×10^6 /mL in a hypotonic fluorochrome solution containing propidium iodide (PI) 50 µg/mL and RNase (10 mg/mL) in 0.1 % sodium citrate plus 0.03 % (v/v) Nonidet P-40. After 60 min at room temperature of incubation, samples were analyzed using a FACSCanto instrument (Becton Dickinson, Montain View, CA, USA). The data were analyzed with Mod.Fit LT 3.3 software. Cell distribution was determined by evaluating the percentage of events accumulated in the different phases of the cycle.

2.7. NF-κB activation

The DNA-binding capacity of NF-κB (p65 subunit) was measured in the nuclear extracts respectively of MCF-7R and MDA-MB-231 cell lines, treated with the TransAM™ NF-κB and Nuclear Extract™ Kits (Active Motif, Carlsbad, CA, USA) according to the manufacturer's instructions. Briefly, the determination is based on the ability of activated NF-κB contained in nuclear extracts to specifically bind an oligonucleotide containing the NF-κB consensus binding site (5′-GGGACT TTCC-3′) immobilized at the bottom of a 96-well plate. Using an antibody directed against an epitope on p65, accessible only when NF-κB is bound to its target DNA, NF-κB bound to the oligonucleotide is detected. The addition of a horseradish peroxidase conjugated secondary antibody provides a sensitive colorimetric readout that is quantified by densitometric analyses. The specificity of the test is confirmed by simultaneous incubations in the presence of an excess of non-immobilized consensus oligonucleotide, as a competitor, or of a mutated consensus oligonucleotide. The results were expressed as arbitrary units: one unit represents the DNA binding capacity shown by 2,5 µg of whole cell extract from Jurkat cells stimulated with 12-O-Tetradecanoylphorbol-13-acetate (TPA) + calcium ionophore (CI)/µg protein of nuclear extracts.

2.8. Invasion assay

Cell migration and invasion assay was performed by CHEMICON Cell Invasion Assay kit using the ECMatrix, reconstituted basement membrane protein matrix (Cat. No. ECM550, Sigma-Aldrich Srl Milan, Italy). Cells were seeded at a density of 4×10^5 cells/well in 6-well plates and cultured for 24 hours, then respectively SEMBL or DHMEQ were added. After 24 hours of treatment, cells were trypsinized, collected and transferred into the transwell chamber with Matrigel, in 500 µL of medium, at a density of 3×10^4. The complete medium was added to the bottom of the chambers. After 24 h of incubation, the cells present in the upper part of the insert (non-migrating cells) were carefully removed from the membrane with a cotton swab, while the cells present in the lower surface of the insert with Matrigel (migrating cells) were treated for 20 min with a dye supplied by the kit. The inserts were washed several times in distilled water and left to dry; cells were then counted under a microscope (CK2 microscope; Olympus, Tokyo, Japan) in 4 randomly selected fields using 40x magnification. Each experiment was performed in duplicate and repeated twice. The results are expressed as % of invasiveness compared to the control (untreated cells). At the same time, an evaluation of cell growth was also carried out in the same treatment conditions.

2.9. Wound healing migration assay

For wound healing assays MCF-7, MCF7-R and MDA-MB-231 cells were seeded in 6 well plate and cultured in routine condition; 10 µL tips were used to perform the wound when the cell density was above 95 %. Then the cells were washed once with fresh medium and cultured in a medium with 1 % of serum, supplemented with SEMBL (0.5 and 1 µg/mL). Images were taken at different time points (0, 24 and 48 h) via an optical microscope (Zeiss AX10, 5X magnification). The wound closure (length) was determined by using Image J software and the percentage wound closure was calculated according to Zhou et al. [10].

2.10. Western blotting

For Western Blotting assays, cell lysates were obtained from both 2D and 3D cultures using RIPA lysis buffer (Santa Cruz Biotechnology Inc., Dallas, TX, USA). 25 µg of proteins were subjected to electrophoretic run on 10 % SDS-PAGE acrylamide gel and then transferred to Hybond-P membrane (GE Healthcare Europe GmbH, Freiburg, Germany). The filters were incubated with GAPDH primary antibodies (1:10000; sc-47724; Santa Cruz Biotechnology, Inc.); MMP-2 (1:2000; #4022 Cell Signaling); E-cadherin (1:2000; #3195 Cell Signaling); Vimentin (1:2000; #5741 Cell Signaling). Hybridization was visualized using an enhanced chemiluminescence detection kit (SuperSignal West Femto Maximum Sensitivity Substrate, Thermo Scientific Life Technologies Italia, Monza, Italy) and the Versa DOC imaging system (BioRad Laboratories, Milan, Italy). Immunoblots were quantified by densitometry using Quantity One software, and the results were expressed as arbitrary units (protein/GADPH).

2.11. Scanning electron microscopy observation

For Scanning Electron Microscopy (SEM) analysis, cell-seeded scaffolds were fixed in 4 % glutaraldehyde at 4 °C for 30 min. Samples were then dehydrated using a series of ethanol solutions (15 %, 35 %, 50 %, 70 %, 95 %, and 100 %) for 3 minutes in each solution and dried at room temperature. Before observation, the samples were placed onto a microscopy stub, sputter coated with gold (Sputtering Scancoat Six, Edwards) for 60 seconds under an argon atmosphere, and observed using a FEG-SEM microscope (QUANTA 200 F, FEI) with an accelerating voltage of 10 kV.

2.12. Zymography

The zymographic analysis was performed on a gelatin substrate supplemented SDS-PAGE gel (10 % acrylamide; 6 mg/mL of gelatin). Cells were grown on 6 well plate for 24 h, then, each cell line, was incubated for further 24 h, respectively with different concentration of

SEMBL or DHMEQ; not treated cells were used as control. After 24 h, the conditioned medium of each sample was recovered and centrifuged at 1200 RPM for 7 min. The supernatant was then freeze-dried and resuspended in 50 μL of fresh medium. Each sample was loaded onto SDS-PAGE gels, and electrophoresis was conducted under nonreducing conditions to maintain enzymatic activity. After the electrophoretic run, gelatin zymograms were incubated for 24 hours at 37 °C in activator buffer containing 2 mM $CaCl_2$, Tris-HCl buffer (50 mM; pH 7.4) containing 1.5 % Triton X-100 and 0.02 % NaN_3, to activate gelatinases. Gels were then stained with Coomassie Brilliant Blue R-250 (Sigma) and destained with methanol and acetic acid solution. Areas of enzymatic activity appeared as clear bands over the dark background. Finally, the acquired image results are analyzed by Quantity One software. The experiment was repeated for two times.

2.13. Immunofluorescent staining and confocal microscopy analysis

MCF-7 cell were grown for 5 days on PLLA scaffold then washed with PBS, fixed with 4 % paraformaldehyde for 15 min at room temperature and permeabilized with 0.1 % Triton X-100 for 10 minutes. The nonspecific sites were saturated with 1 % bovine serum albumin (BSA) for 1 hour at room temperature. Cells were incubated with anti-Vimentin (1:100, D21H3 Cell Signaling) overnight at 4 °C. The next day, cells were richly washed with PBS and incubated with Rabbit TRITC secondary antibody (1:200, T6778 Sigma-Aldrich) for 1 hour at room temperature. After richly washing with PBS cells were incubated with Phalloidin-FITC (1:1000, P5282 Sigma-Aldrich) for 1 hour at room temperature to label the actinic cytoskeleton and with DAPI (1:20.000, Sigma-Aldrich D9542) to label nucleus and observed using a confocal laser scanning microscope with a 60x magnification (Olympus FluoView10i).

2.14. Realtime PCR

Total RNA was extracted from MDA-MB-231 and MCF-7 cells with TRIzol reagent (Life Technologies) following the manufacturer's instructions. RNA concentration was measured with a spectrophotometer (Thermo Scientific, MA) and cDNA was synthesized with reverse transcription kit (Applied Biosystems Life Technologies Inc., Foster City, CA, USA). For 3D experiments: Real-time quantitative polymerase chain reaction (qPCR) was performed with the TaqMan Gene Expression Master Mix kit (Applied Biosystems Life Technologies Inc., Foster City, CA, USA) in triplicates. The PCR cycling conditions were as follows: Denaturation at 50 °C for 2 min, annealing at 95 °C for 10 min, followed by 40 cycles of 95 °C for 15 s and extension at 60 °C for 60 min. The specific primers used were Vimentin Hs00185584_m1 and GAPDH Hs99999905_m1 (Applied Biosystems Life Technologies Inc., Foster City, CA, USA). Relative expression was calculated using the comparative Ct method [ΔCt = Ct (target gene) – Ct (housekeeping gene)]. Where Ct was the fractional cycle number at which the fluorescence of each sample passed the fixed threshold. Fluorescence was measured at 515–518 nm using StepOne AB Real Time PCR System software (Applied Biosystems Life Technologies Inc., Foster City, CA, USA). For quantitative expression analysis of Vimentin, E-cadherin and MMP-2 (2D and 3D) BrightGreen 2X qPCR MasterMix (Applied Biological Materials Inc. Richmond, BC V6V 2J5 Canada) was employed to analyze the obtained cDNA in triplicates. The running of the samples and data collection were performed on a StepOne AB Real Time PCR system (Applied Biosystems Life Technologies Inc., Foster City, CA, USA). The qRT-PCR was performed using the primers: β-Actin F-CGGGAAATCGTGCGTGACAT and β-Actin R-GGACTCCATGCCCAGGAAGG; MMP-2 F -TACAGGATCATTGGCTACACACC and MMP-2 R-TATCCATCGCCATGCTCCCAG; Vimentin F-CAGGACTCGGTGGACTTCTC and Vimentin R-TAGTTGGCGAAGCGGTCATT; E-cadherin F-GAGAACGCATTGCCACATACA and E-cadherin R-ACCTTCCATGACAGACCCCTTAA. β-Actin was used as an internal standard. The running of the samples and data collection were performed on a StepOne AB Real Time PCR system (Applied Biosystems Life Technologies Inc., Foster City, CA, USA).

2.15. Statistical analysis

The results obtained are reported as mean ± standard error (SE). Statistical analysis was performed by analysis of variance (one-way ANOVA) followed by Tukey's test. STATISTICS ver. 10 (StatSoft Inc. 2011) was used as the analysis software.

3. Results

3.1. Antiproliferative activity of SEMBL in breast cancer cell lines

The cytotoxic activity of SEMBL was evaluated in the three breast cancer cell lines, by MTS assay, respectively after 24, 48 and 72 h of treatment. Table 1 shows the IC_{50} values (concentration which inhibits 50 % of cell growth), while Fig. 1 refers to the cytotoxicity curves obtained in the cell lines after 72 hours of treatment. SEMBL is more potent than the parent compound DHMEQ, showing IC_{50} significantly lower (Table 2). Cytotoxicity assay conducted on 1–7HB2, a non-tumor cell line, shows an $IC_{50} > 10$ μg/mL indicating that SEMBL is not cytotoxic in the concentration range used for tumor cells.

To analyze the role of SEMBL in the cell cycle and the type of cell death induced, we treated the different cell lines at the corresponding IC_{50} values and performed a flow cytometric analysis. In particular, SEMBL determines necrotic cell death on all cell lines (Table 3). After 72 h of treatment, the cell cycle analysis shows a modest increase of cells in the G2 phase compared to controls (Table 4).

The results are expressed as relative cell death values of the three cell lines after treatment with SEMBL at 24, 48 and 72 h, compared to controls (mean ± standard error of two different experiments).

The results are expressed as percentages of distribution in cell cycle phases of the three cell lines after treatment with SEMBL at 72 h (mean ± standard error of two different experiments).

3.2. Effects of SEMBL on NF-κB (p65 Subunit) DNA binding capacity

Our previous data indicated that the MCF-7 cell line exhibited very slight DNA binding capacity of the p65 subunit [11]. Otherwise, the MCF-7R and MDA-MB-231 cell lines showed remarkable levels of the activated p65 subunit [11,12]. To verify the ability of SEMBL to interfere with the DNA binding capacity of NF-κB (p65 subunit) in the considered BC models, we analyzed its effects on NF-κB activation by TransAM™ assay. The MDR cell lines were treated with SEMBL (IC_{50} and IC_{70} values) or DHMEQ (IC_{50}) for 24 hours. As shown in Fig. 2, SEMBL resulted in a significant decrease in the binding capacity of NF-κB to the corresponding DNA consensus sequence with a strong effect compared to that shown by DHMEQ.

3.3. SEMBL-mediated inhibition of invasive capacity

To evaluate the degree of aggressiveness of the three different cell lines, after treatment with SEMBL, a cellular invasiveness assay was performed using ECMatrix chambers. The cells were treated for 24 hours respectively, with SEMBL concentration lower than its IC_{50}, and with the reference drug DHMEQ, used at a concentration 10 times higher than

Table 1
IC_{50} values after 24, 48 and 72 h of treatment with SEMBL in the three different cell lines.

	IC_{50} ± SE (24 h)	IC_{50} ± SE (48 h)	IC_{50} ± SE (72 h)
MCF−7	6.5 μg/mL ± 0.46	7.0 μg/mL ± 0.18	2.5 μg/mL ± 0.39
MCF−7R	4.7 μg/mL ± 0.39	4.0 μg/mL ± 0.11	3.8 μg/mL ± 0.14
MDA-MB−231	4.5 μg/mL ± 0.35	3.2 μg/mL ± 0.18	1.4 μg/mL ± 0.02

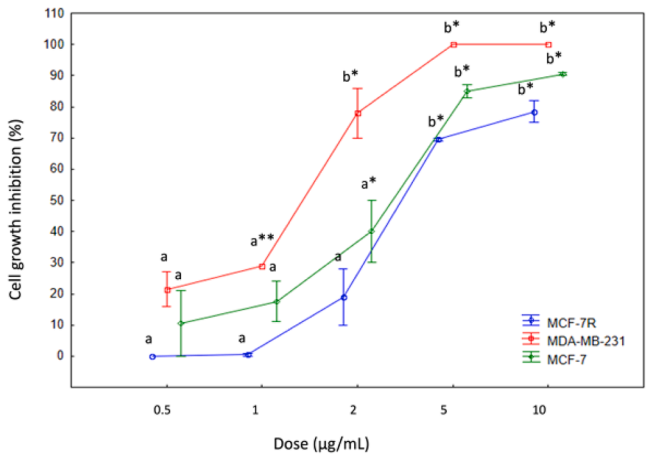

Fig. 1. Antiproliferative activity of SEMBL evaluated by MTS assay on the three cell lines. The results are expressed as the mean ± standard error of two experiments performed in triplicate. *p < 0.05 and **p < 0.01 treatments vs control; the different letters represent the significant differences between the different concentrations of SEMBL (Tukey test, p < 0.01).

Table 2
IC_{50} values after 72 h of treatment with DHMEQ in the three different cell lines.

	IC_{50} ± SE
MCF−7	27.5 μg/mL ± 0.46*
MCF−7R	31.0 μg/mL ± 0.7**
MDA-MB−231	34.0 μg/mL ± 1.1**

* p < 0.005
** p < 0.001 IC_{50} DHMEQ vs IC_{50} SEMBL.

Table 3
Cell death of the three different cell lines, control and after treatment with SEMBL.

	Cell death		
	24 h	**48 h**	**72 h**
MCF−7	1	1	1
MCF−7 μg/mL	1.45 ± 0.1	1.40 ± 0.07	1.30 ± 0.07
MCF−7R	1	1	1
MCF−7R μg/mL	2.35 ± 0.2	1.80 ± 0.07	1.11 ± 0.09
MDA-MB−231	1	1	1
MDA-MB−231 μg/mL	2.22 ± 0.1	3.65 ± 0.4	2.35 ± 0.1

Table 4
Cell distribution in different phases of the cell cycle, control and after treatment with SEMBL.

	G1 (%)	G2 (%)	S (%)
MCF−7	85.1± 0.5	0.5 ± 0.3	14.4 ± 0.8
MCF−7 + SEMBL (2.5 μg/mL)	77.6 ± 1.0	2.9 ± 1.8	19.5 ± 0.8
MCF−7R	56.7 ± 0.5	0.7 ± 0.5	42.6 ± 0.0
MCF−7R + SEMBL (3.8 μg/mL)	50.9 ± 1.3	1.1 ± 0.07	48.0 ± 1.3
MDA-MB−231	72.6 ± 2.5	3.5 ± 2.5	24.2 ± 0.4
MDA-MB−231 + SEMBL (1.4 μg/mL)	72.8 ± 0.3	5.3 ± 0.0	21.8 ± 0.3

SEMBL. The results shown in Fig. 3, indicated a clear reduction in the invasive capacity of all three cell types examined obtained with SEMBL, confirming greater potency compared to DHMEQ also in terms of anti-metastatic activity.

3.4. Wound healing migration assay

In addition to the invasiveness assay, the migration test was performed, to evaluate the wound healing capacity of the cell monolayer. The three cell lines were seeded on a plate and a scratch-made upon reaching 95 % confluence. The cells were rinsed thoroughly to remove detached cells and treated with two sub-cytotoxic concentrations of SEMBL (0.5 μg/mL and 1 μg/mL). The images of the culture were taken under an optical microscope at time 0, 24 and 48 h. The results are expressed as a percentage of wound closure compared to the untreated control. Cells treated with SEMBL showed a lower migration ability and in a dose-dependent manner compared to control cells (Fig. 4).

Table 5 shows the migration rate after 24 and 48 h of treatment with SEMBL (0.5 and 1 μg/mL) in the three different cell lines.

3.5. Modulation of factors involved in cell migration and invasiveness

To validate the results obtained with the invasiveness and migration assays, the action of SEMBL was evaluated on the expression level of protein involved in the migration and invasiveness processes. A Western Blotting assay was performed after treatment of the three cell lines with SEMBL at concentrations corresponding to the IC_{50} and IC_{70} and with DHMEQ (IC_{50}) for 24 h. Based on the literature [6] which indicated a specific action of SEMBL on metalloproteinase 2 (MMP-2), its expression and that of Vimentin and E-cadherin were evaluated. Vimentin as a positive marker of the EMT process, was expressed only in MDR cell lines, while E-cadherin was not expressed in MCF-7R cells.

The results shown in Fig. 5 confirmed a strong inhibitory action of SEMBL on MMP-2 in the MCF-7 cell line, where it appears to be dose-dependent, and in its MDR variant cell line. SEMBL downregulated the expression of Vimentin in MCF-7R cells and upregulated the expression of E-cadherin in the parental cell line. In the MDA-MB-231 cell line, the results showed an inhibitory action of SEMBL on Vimentin only at the highest dose while a dose-dependent increase was shown in the expression of E-cadherin. DHMEQ seems to have a lower action compared to that of the SEMBL. To verify that MMP-2 was enzymatically active, and to confirm the modulation of SEMBL also on its enzymatic activity, a zymographic analysis was carried out on media conditioned by the respective cell lines. As shown in Fig. 6 is possible to observe the two bands relating to the pro-form and the active form of MMP-2 and a reduction of MMP-2 activity under treatment of SEMBL and DHMEQ.

To corroborate the data of Western Blotting analysis, qRT-PCR was performed. Overall, the modulation of MMP-2, E-cadherin and Vimentin induced by SEMBL and DHMEQ at mRNA levels is comparable to that observed at protein levels (Fig. 7).

3.6. Antiproliferative activity of SEMBL on 3D models

The cytotoxic activity of SEMBL was evaluated in the three BC cell lines seeded on PLLA scaffold, by MTS assay, after 72 h of treatment. In the Table 6 are shown the IC_{50} values, that resulted 10- fold higher than those obtained in 2D cell lines.

SEM analysis confirmed the MTS results. Fig. 8 (A-C) shows the cell morphologies detected, for the three cell types, in the controls (i.e., cells grown in not treated medium). It is easy to notice that MDA-MB-231 cells grew into the scaffold by assuming a conformation characterized by several cell aggregations with an irregular three-dimensional cell morphology. On the other hand, the MCF-7 cells formed a well-defined continuous layer onto the scaffold surface. Very different conditions were observed in the samples grown in the media containing a drug concentration higher than IC_{50} (Fig. 8: D-F). Very few MDA-MB-231 cells were detected in the scaffolds and the layer of MCF-7 is almost disappeared.

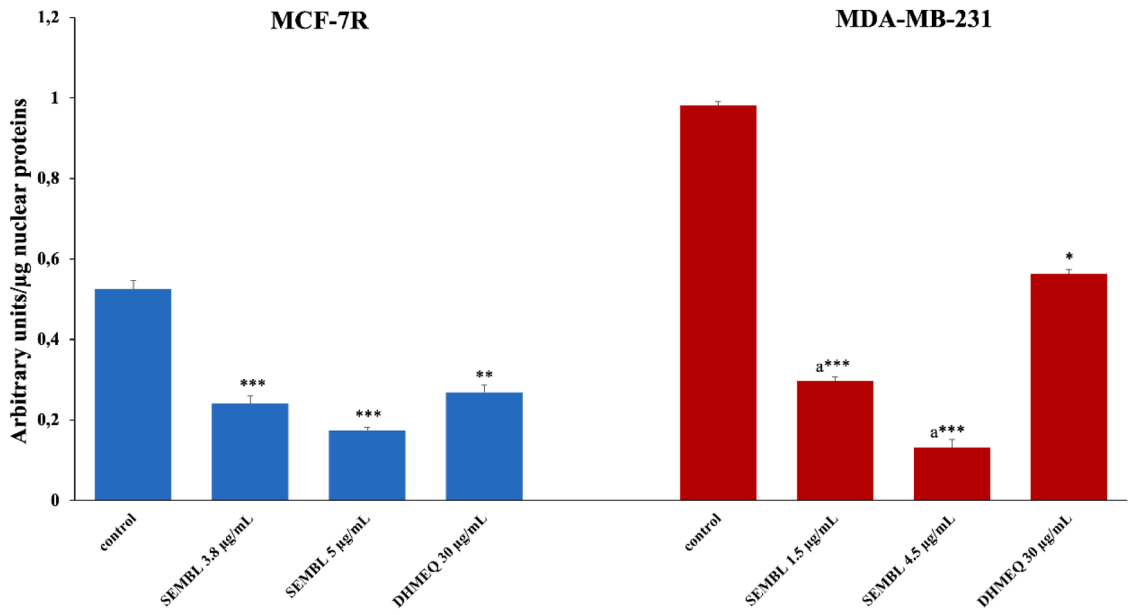

Fig. 2. DNA binding capacity of NF-κB (p65 subunit) in nuclear extracts of MCF-7R and MDA-MB-231 cells. Cells were treated for 24 h with SEMBL (IC_{50} and IC_{70} values) or DHMEQ (IC_{50}). Results are expressed as arbitrary units/µg of cell nuclear extract protein. Differences when treatments are compared to control: *p<0.05, **p<0.01 and ***p<0.005, ^{a}p <0.05 SEMBL vs DHMEQ (Tukey's test).

3.7. Modulation of factors involved in cell migration and invasiveness in 3D models

The effects of SEMBL on proteins involved in migration and invasiveness were evaluated also on 3D models by Western blotting analysis. The three BC cell lines seeded on PLLA scaffold were treated with SEMBL at concentrations corresponding to the $IC_{50,}$ for 24 h. In Fig. 9 were shown the results on MMP-2, Vimentin and E-cadherin expression. SEMBL was able to modulate the expression of the factors involved in the EMT process on 3D models, confirming its anti-metastatic potency. As we have seen before, in the 2D condition, Vimentin expression was observed only in MCF-7R and MDA-MB-231, but not on MCF-7 cells. Since Vimentin levels are positively associated with a loss of epithelial tracts and a gain of a pro-migratory mesenchymal phenotype, growth in 3D conditions on the scaffold favors the expression of a more invasive phenotype. It is interesting to note that Western blotting analysis shows Vimentin expression in MCF-7 cells grown in PLLA scaffolds. To evaluate whether Vimentin expression can be influenced by growth modality (2D vs. 3D), the cell grown in PLLA scaffold for 5 days were analyzed by confocal microscopy after staining with a Vimentin antibody. To confirm the Western blotting data, the expression of Vimentin on the 3D model was then verified by further analysis. As observed by confocal microscopy analysis, (Fig. 10 A) MCF-7 cells cultured in PLLA scaffolds for 5 days, show Vimentin expression in the perinuclear region which comigrates with phalloidin, both marking the cytoskeleton. In Fig. 10 B, Vimentin mRNA expression level was confirmed by qRT-PCR, using as control MDA-MB-231cells, which constitutively express Vimentin.

The results of qRT-PCR confirmed those of Western Blotting analyses (Fig. 11). Regarding the MCF-7R cell line in 3D, MMP-2 mRNA expression appears not relevant.

4. Discussion

The synthesis of DHMEQ by Prof. Umezawa about 20 years ago was a decisive step in the discovery of an irreversible NF-κB inhibitor. DHMEQ, in fact, can bind to NF-κB components covalently and independently of the event that determines its activation. Despite the numerous studies that confirm the high therapeutic power of DHMEQ as an anti-tumor and anti-inflammatory *in vitro* and *in vivo*, its great limit is represented by its instability in the body. It is easily degraded in the blood and for this reason not applicable for intravenous administration. At present, an ointment for topic administration is being developed in the industry [4]. Based on these premises, Prof. Umezawa have synthesized a more stable compound derived from DHMEQ with the same mechanism of action. (S)-b-salicyloylamino-a-exo-methylene-γ-butyrolactone (SEMBL), the epoxide-free analog of DHMEQ, is also more potent than DHMEQ, in inhibiting NF-κB activation and reducing cell proliferation in mouse monocytic leukemia RAW264.7 cells; furthermore, it also shows an inhibitory effect on the cellular migratory capacity, with a specific action on the expression of matrix metalloproteinase 2 (MMP-2) in the clear cells of ovarian carcinoma ES-2 cells [6,13]. To our knowledge, its antitumor and antimigratory activities in other neoplastic disease have not been evaluated. We chose breast cancer as a study model. Given the great heterogeneity, there is a wide range of therapeutic options concerning invasive capacity and positivity/negativity for hormone receptors. Alongside the now standardized protocols and numerous targeted therapies [14,15], there are new perspectives such as the vaccines for the HER-2^{+} subtypes (GP2 and AE37) in phase II of a clinical trial that has shown encouraging results [16] or sacituzumab govitecan, approved by FDA for the treatment of adult patients with metastatic or unresectable triple-negative breast cancer who have received at least two prior systemic therapies with at least one for advanced disease. Unfortunately, there is a high rate of death related to adverse events in breast cancer survivors, such as cardiac diseases, leukemia, lung cancer and esophageal cancer [17]. Furthermore, invasive tumors with the high rate of metastasis in various organs cause a drastic increase in the percentage of death [18]. The metastatic process involves sequential and interconnected steps during which tumor cells, supported by an increase in angiogenic processes, develop invasive growth. They detach from the primary tumor, break the vessel wall, migrate into the circulatory system, and evade the attack of the immune system; thereby they degrade the basal membrane, invading and proliferating in distant organs. The prognosis of metastatic breast cancer does not depend only on a late diagnosis but also on other factors such as age, ethnicity, endogenous hormones, menopause, smoking, first-degree relatives, mutations, and grade and size of the primary tumor [19–21]. Moreover, the five different biological subtypes (human epithelial growth receptor type 2 (HER2), luminal A, luminal B,

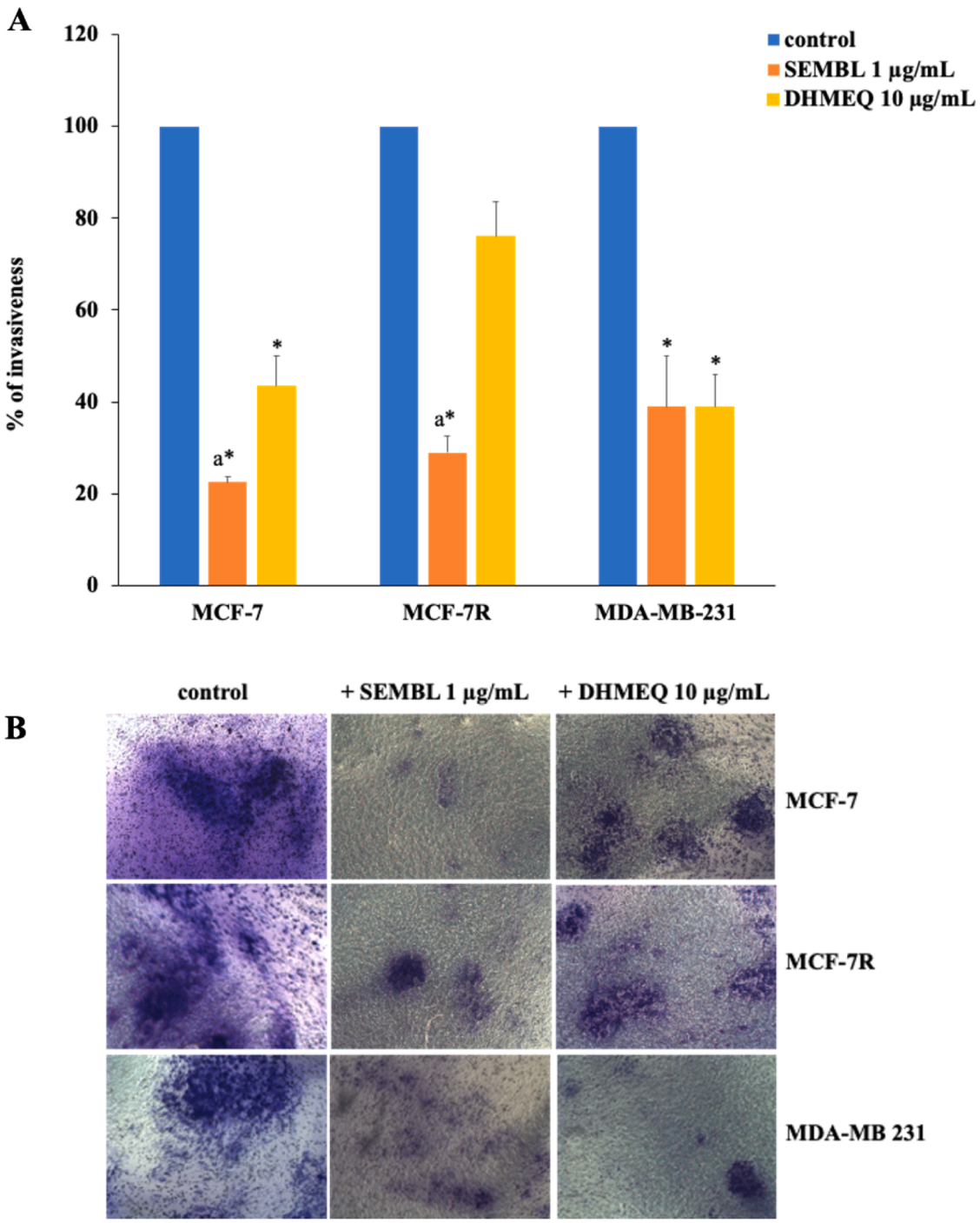

Fig. 3. Invasion assay. Cells were treated for 24 h with SEMBL (1 µg/mL) and DHMEQ (10 µg/mL). The assay was conducted using the 24-well Transwell chamber. **A.** The results are expressed as % invasiveness compared to the untreated control and are the mean ± standard error of two experiments. *$p < 0.01$ treatments vs control. [a]$p < 0.05$ of SEMBL vs DHMEQ (Tukey's test). **B.** Representative analysis by matrigel assay of the evaluation of cell invasiveness 24 h after treatment with SEMBL 1 µg/mL and DHMEQ 10 µg/mL.

claudin-low, and basal-like) show different abilities to metastasize to distant organs, specific pathways with the preferred metastatic sites, and different survival response after relapse [22,23]. The inhibition of the metastasis process, which in most cases is responsible for the poor outcome of all therapies, would allow to attack a tumor mass in situ by surgery and/or radiation and drug therapy, with a higher probability of success.

In the present paper we examined the anticancer properties and the ability to reduce the metastatic potential of SEMBL in three BC cell models reflecting the most frequently observed histotypes. In particular, the study was performed on adenocarcinoma cell line, MCF-7, on its MDR variant, MCF-7R cells, and on triple negative breast cancer cell line, MDA-MD-231. Although there are different invasiveness processes, our study focused on the EMT process which would appear seems to be the one carried out by our cancer models. During the EMT, tumor cells lose their epithelial features and acquire a mesenchymal phenotype leading to invasive and migratory behavior. The earliest events of the EMT include the downregulation of cell-cell adhesion molecules, such as the adherens junction protein E-cadherin, and upregulation of weak adhesion related molecules, such as N-cadherin and Vimentin. In

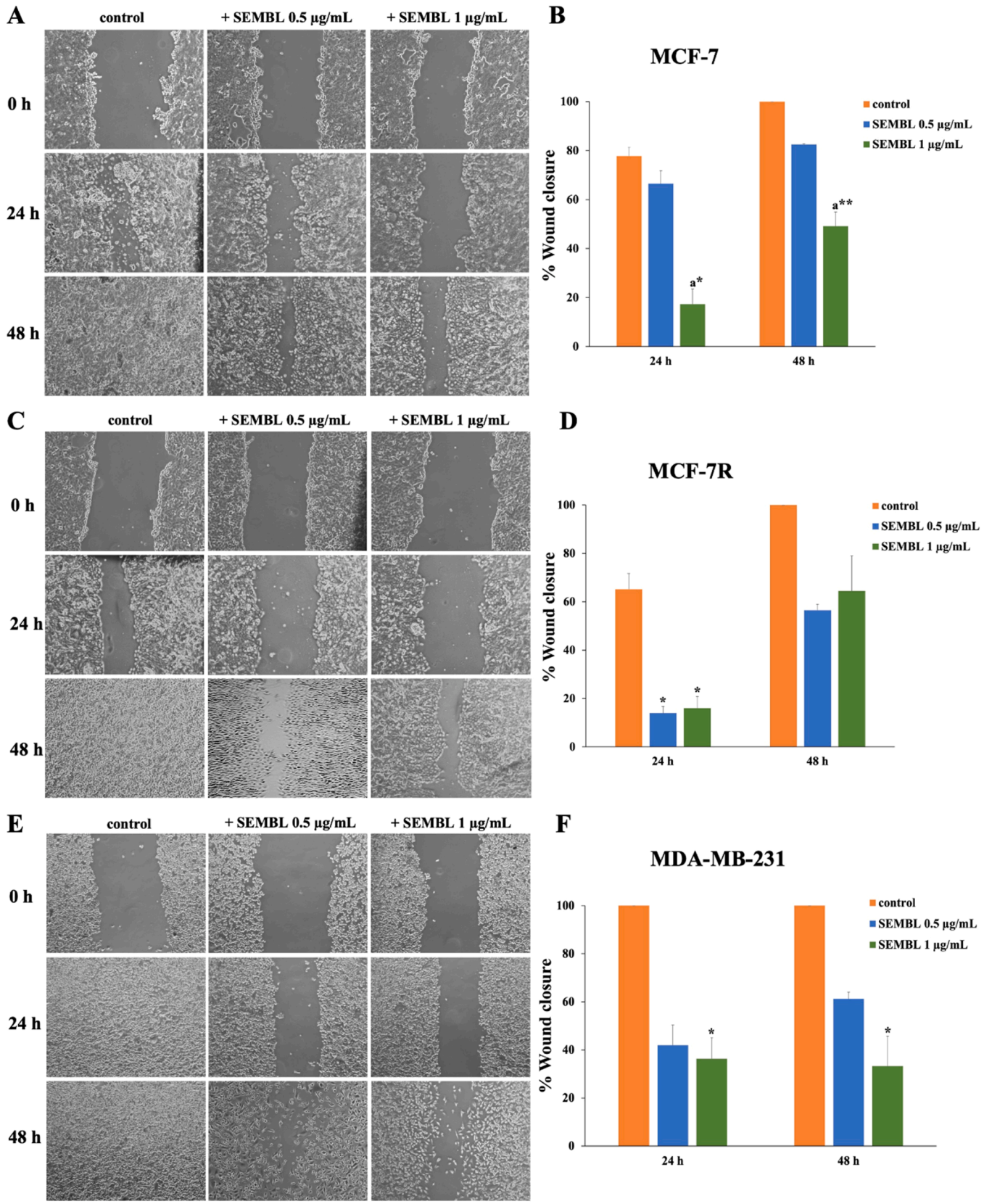

Fig. 4. Wound healing test. Representative images of the Wound healing tests in MCF-7 **(A)** MCF-7R **(C)** and MDA-MB-231 **(E)** cell lines; assessment of cell migration at 24 and 48 h after SEMBL treatment (0.5 µg/mL and 1 µg/mL); **(B, D** and **F)** the results are expressed as % wound closure compared to the untreated control and are the mean ± standard error of two experiments, and F) compared to the untreated control and are the mean ± standard error of two experiments **p< 0.01, *p< 0.05 vs control, [a]p < 0.05 SEMBL 1 µg/mL vs SEMBL 0.5 µg/mL (Tukey's test).

Table 5
The migration rate (μm/h) in the three different cell lines.

Cell lines	Time (h)	Migration rate μm/h (media ± SE)		
		Control	+SEMBL 0.5 μg/mL	+SEMBL 1 μg/mL
MCF−7	24	8.25 ± 0.20	7.32 ± 1.0	1.35 ± 0.47[a*]
	48	5.13 ± 0.09	4.51 ± 0.31	2.24 ± 0.03[b**]
MCF−7R	24	8.07 ± 1.30	1.53 ± 0.44	1.89 ± 0.58
	48	6.07 ± 0.44	3.01± 0.43	3.81 ± 0.86
MDA-MB−231	24	10.83 ± 0.35	4.21 ± 0.76	3.64 ±1.20
	48	5.42 ± 0.18	3.08 ± 0.09	1.71 ± 0.80

Each value represents the mean ± standard error of two experiments, **p<0.01 and *p<0.05 *vs* control, [a]p<0.005 and [b]p<0.01 SEMBL 1 μg/mL *vs* SEMBL 0.5 μg/mL.

addition, matrix metalloproteinases (MMPs), which can degrade the extracellular matrix (ECM), are upregulated [24]. SEMBL shows anti-proliferative and antimigratory effects, NF-κB and MMP-2 inhibition mediated, in all cell lines. These effects occur at concentrations significantly lower than the reference compound, confirming the greater potency of SEMBL compared to DHMEQ also in BC cellular models.

Monolayer cultures are easy to manipulate and cost-effective but lack the complex structure and cellular interactions typical of tumors. As a result, 2D cultures often oversimplify the study of cancer biology and may not accurately represent the response of cancer cells to potential therapies. In recent years polymeric structure called "scaffolds" enabled researchers to culture cancer cells in a 3D environment that closely mimics the *in vivo* environment in terms of cell-cell and cell-matrix interactions, so the scaffolds became a novel suitable candidate to be a 3D *in vitro* model for cancer research [25]. For this purpose, the results obtained on 2D models were corroborated by analyzes performed on 3D models made up of PLLA scaffolds made by Thermally Induced Phase Separation (TIPS) technique [26,27]. Our data indicated that cell growth in the scaffold promotes Vimentin expression, which plays a pivotal role in the ability of cells to invade their surrounding matrix. This is of particular interest in cancer, where, the acquisition of a motile phenotype and invasive capacity leads to metastases, the main cause of death in cancer patients. Vimentin intermediate filaments are very important for the elongation and maturation of invadopodia, which are essential for generating the pressure that drives cell migration in the 3D environment [28]. Since cancer cell motility through the extracellular matrix is the first and essential step of the metastatic process, the importance of Vimentin in EMT and other processes involved in cell motility makes it an attractive migrastatic drug target [29].

5. Conclusion

In summary, this work, in addition to highlighting the anti-proliferative and anti-migratory potential of SEMBL on three different breast cancer cell lines, also underline that PLLA biocompatible supports constitute a valid 3D study model. The fact that SEMBL is able to reduce its expression on both 2D and 3D cell cultures appears to be a significant outcome.

Author agreement statement

The authors declare that this manuscript is original, has not been published before and is not currently being considered for publication elsewhere. They confirm that the manuscript has been read and

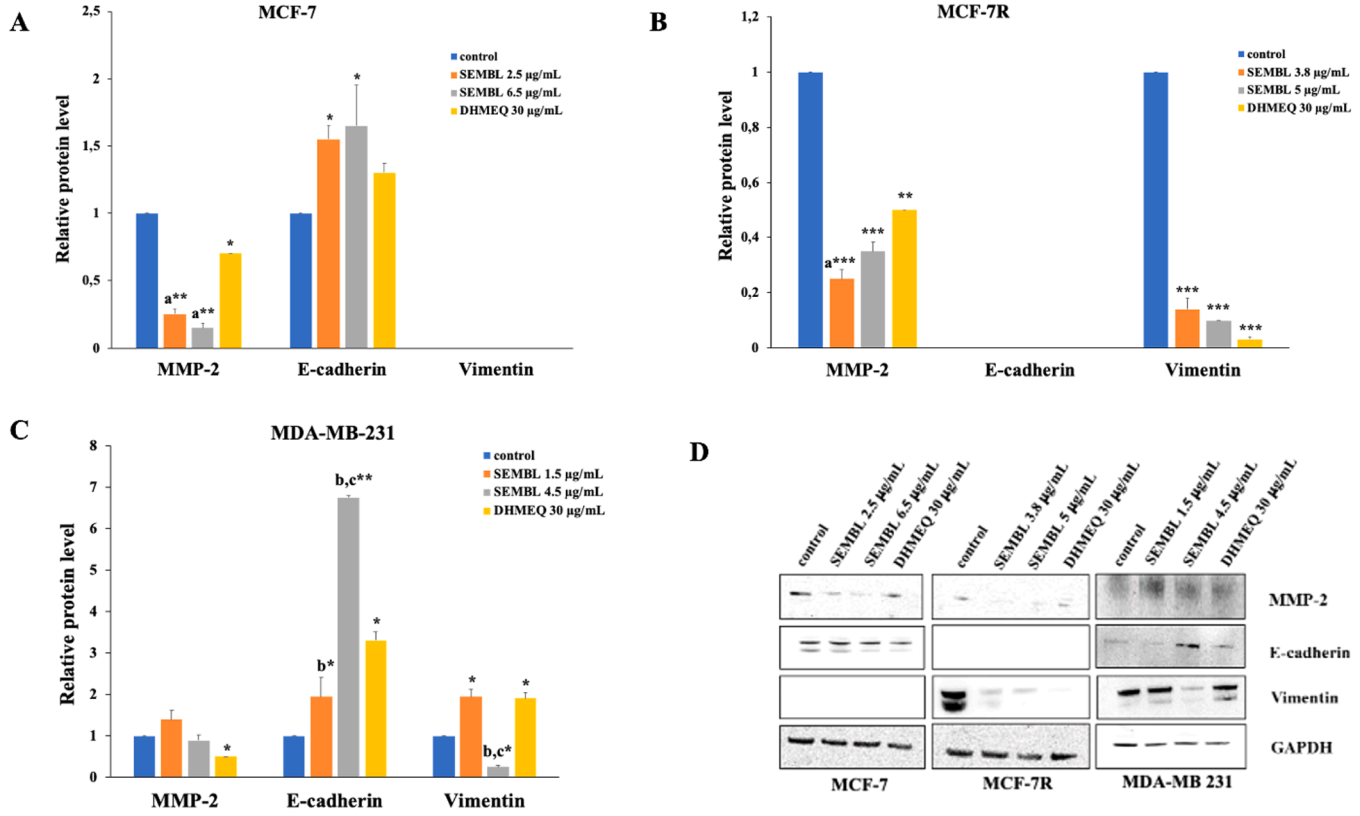

Fig. 5. Western blotting analysis of MMP-2, E-cadherin and Vimentin levels. **A.** MCF-7 cells treated for 24 h with SEMBL (2.5 and 6.5 μg/mL) and DHMEQ (30 μg/mL); **B.** MCF-7R cells treated for 24 h with SEMBL (3.8 and 5 μg/mL) and DHMEQ (30 μg/mL); **C.** MDA-MB-231 cells treated for 24 h with SEMBL (1.5 and 4.5 μg/mL) and DHMEQ (30 μg/mL). The results are expressed as the mean ± standard error of two different experiments. Differences when treatments are compared to control: ***p<0.001 **p<0.01, *p<0.05; differences when treatments are compared with each other: [a]p <0.05 SEMBL vs DHMEQ, [b]p < 0.01 SEMBL vs DHMEQ, [c]p < 0.01 SEMBL 4.5 μg/mL vs SEMBL 1.5 μg/mL (Tukey's test). **D.** Results of a representative experiments. C: control, S: SEMBL, **D:** DHMEQ.

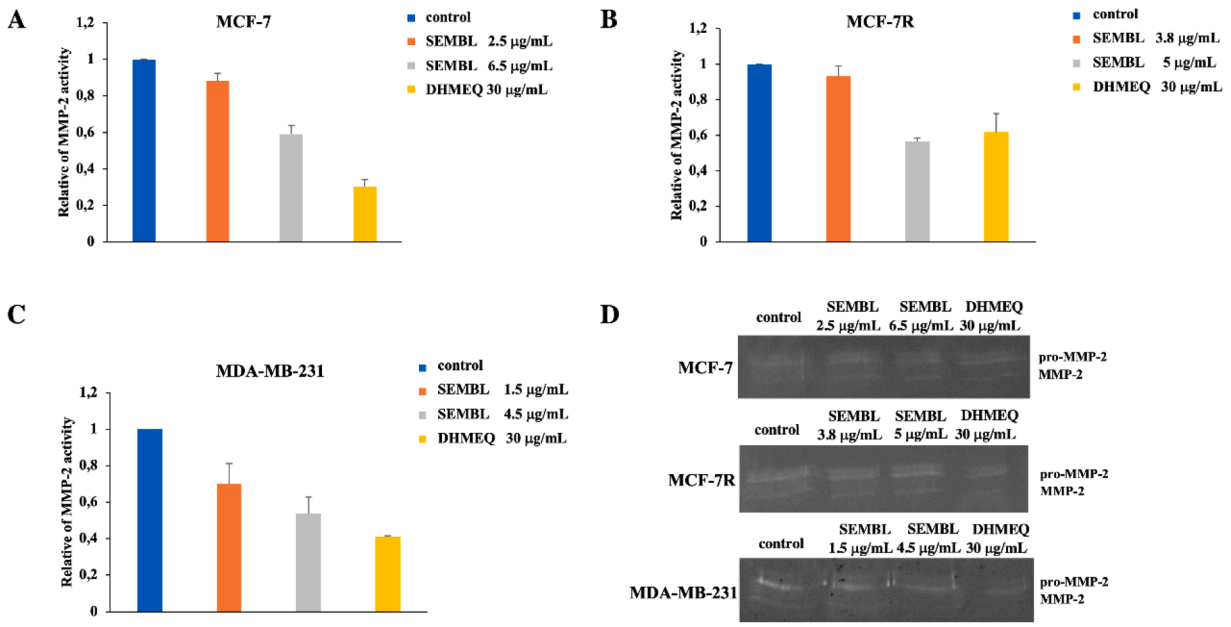

Fig. 6. Effect of SEMBL and DHMEQ on the activity of MMP-2. Quantitative analysis of active-MMP-2 in breast cancer cells. **A.** MCF-7 cells treated for 24 h with SEMBL (2.5 and 6.5 µg/mL) and DHMEQ (30 µg/mL); **B.** MCF-7R cells treated for 24 h with SEMBL (3.8 and 5 µg/mL) and DHMEQ (30 µg/mL); **C.** MDA-MB-231 cells treated for 24 h with SEMBL (1.5 and 4.5 µg/mL) and DHMEQ (30 µg/mL). The results are expressed as the mean ± standard error of two different experiments. Differences when treatments are compared to control: ***p<0.005, **p<0.01, *p<0.05 (Tukey's test). **D.** Representative gelatin zymograms of MCF-7, MCF-7R and MDA-MB-231 cell lines. C: control, S: SEMBL, D: DHMEQ.

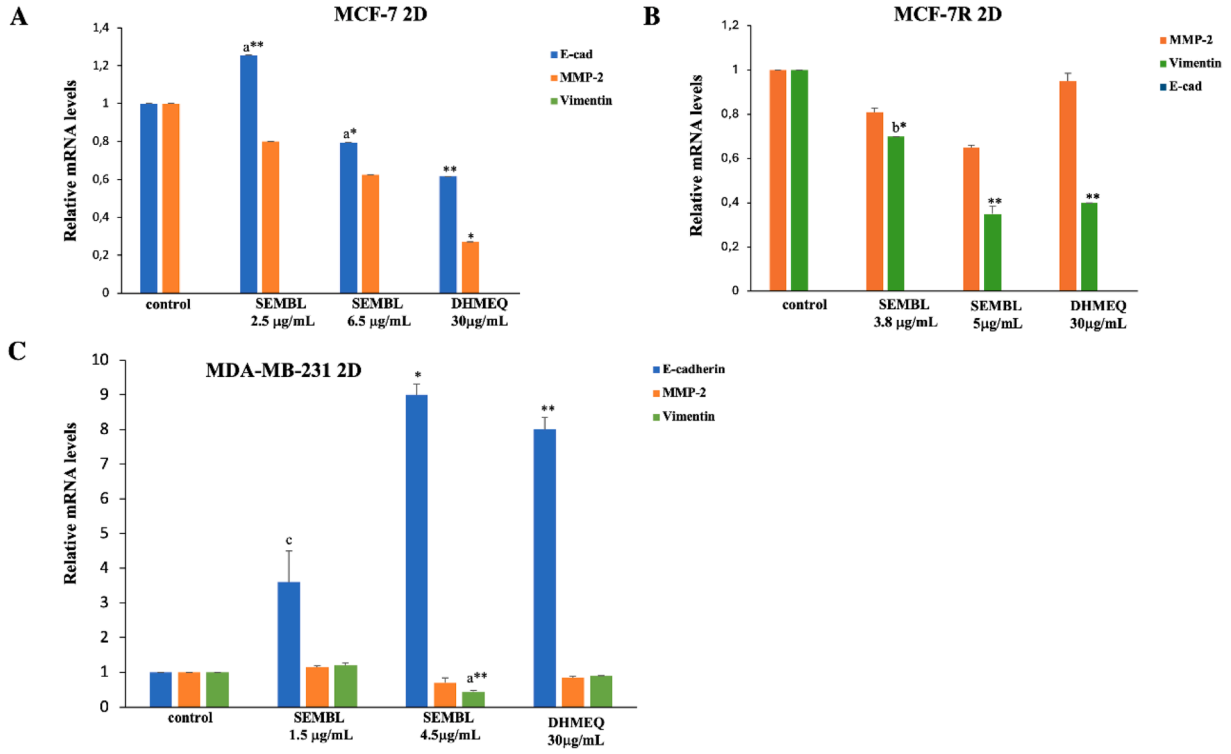

Fig. 7. Evaluation of MMP-2, E-cadherin and Vimentin mRNA expression levels by qRT-PCR. For each condition, N=3 technical replicates were used. Data are expressed as mean ± standard error of two experiments. In particular, cells were treated as well as for protein expression detection: **A.** MCF-7 cells treated for 24 h with SEMBL (2.5 and 6.5 µg/mL) and DHMEQ (30 µg/mL); **B.** MCF-7R cells treated for 24 h with SEMBL (3.8 and 5 µg/mL) and DHMEQ (30 µg/mL); **C.** MDA-MB-231 cells treated for 24 h with SEMBL (1.5 and 4.5 µg/mL) and DHMEQ (30 µg/mL). Differences when treatments are compared to control: **p<0.005, *p<0.05; differences when treatments are compared with each other: ^{a}p <0.05 SEMBL vs DHMEQ, ^{b}p <0.005 SEMBL vs DHMEQ, ^{c}p <0.01 SEMBL vs DHMEQ (Tukey's test). C: ^{c}ontrol, S: SEMBL, D: DHMEQ.

Table 6
IC_{50} values after treatment with SEMBL in the 3D BC cell lines.

	IC_{50} ± SE
MCF−7	20.0 μg/mL ± 0.35
MCF−7R	32.5 μg/mL ± 1.8
MDA-MB−231	13.0 μg/mL ± 1.7

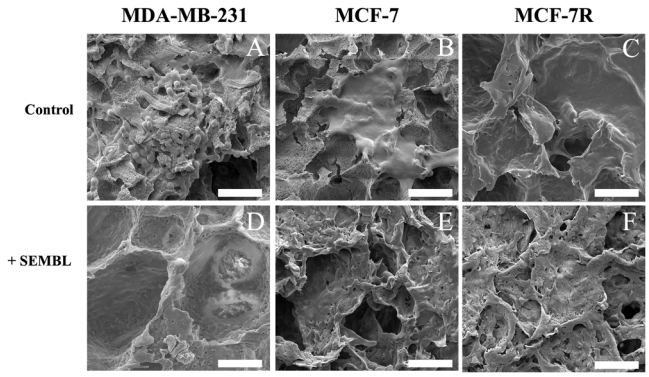

Fig. 8. SEM micrographs of the cross sections of PLLA scaffolds. (A-C) scaffold with cells grown in normal medium. (D-F) scaffold with cells grown in medium containing a concentration of SEMBL higher than IC_{50}. Scale bar 50 μm.

approved by all named authors and that there are no other persons who satisfied the criteria for authorship but are not listed. They further confirm that the order of authors listed in the manuscript has been approved by all of us. They understand that the Corresponding Author is the sole contact for the Editorial process. She is responsible for communicating with the other authors about progress, submissions of revisions and final approval of proofs.

Funding

This work was supported by: FFR-DR-160829 to Monica Notarbartolo; FFR-DR15–161507 to Paola Poma, FFR-DR15–180400 to Manuela Labbozzetta, University of Palermo, Italy; Project partially financed by the European Union – Next Generation EU- Overcoming transporter-mediated cancer multidrug REsistance by innovative pharmacological And physiCal sTrategies (REACT) [2022X7ESJ3-CUP B53D23020820006].

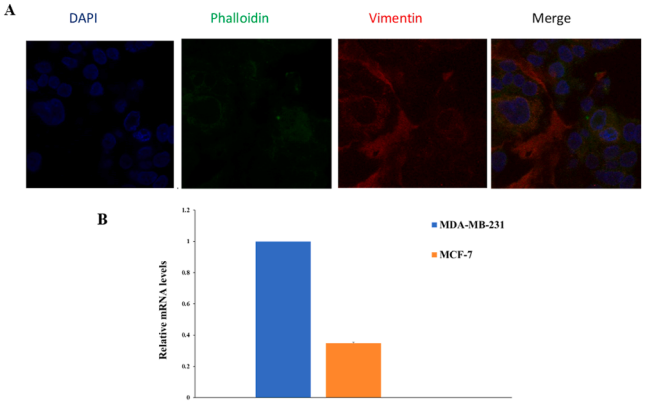

Fig. 10. Expression of Vimentin in 3D MCF-7 cell line. **A.** Confocal microscopy analysis of MCF-7 cell after 5 days of cell growth in tridimensional condition (nuclei blue DAPI, cytoskeleton green Phalloidin and red anti-Vimentin), magnification 60x. **B.** Evaluation of Vimentin mRNA expression levels by qRT-PCR. For each condition, N=3 technical replicates were used. Data are expressed as mean ± standard error of three experiments. mRNA from MDA-MB-231 cells was used as a positive control to which an arbitrary unit value was assigned.

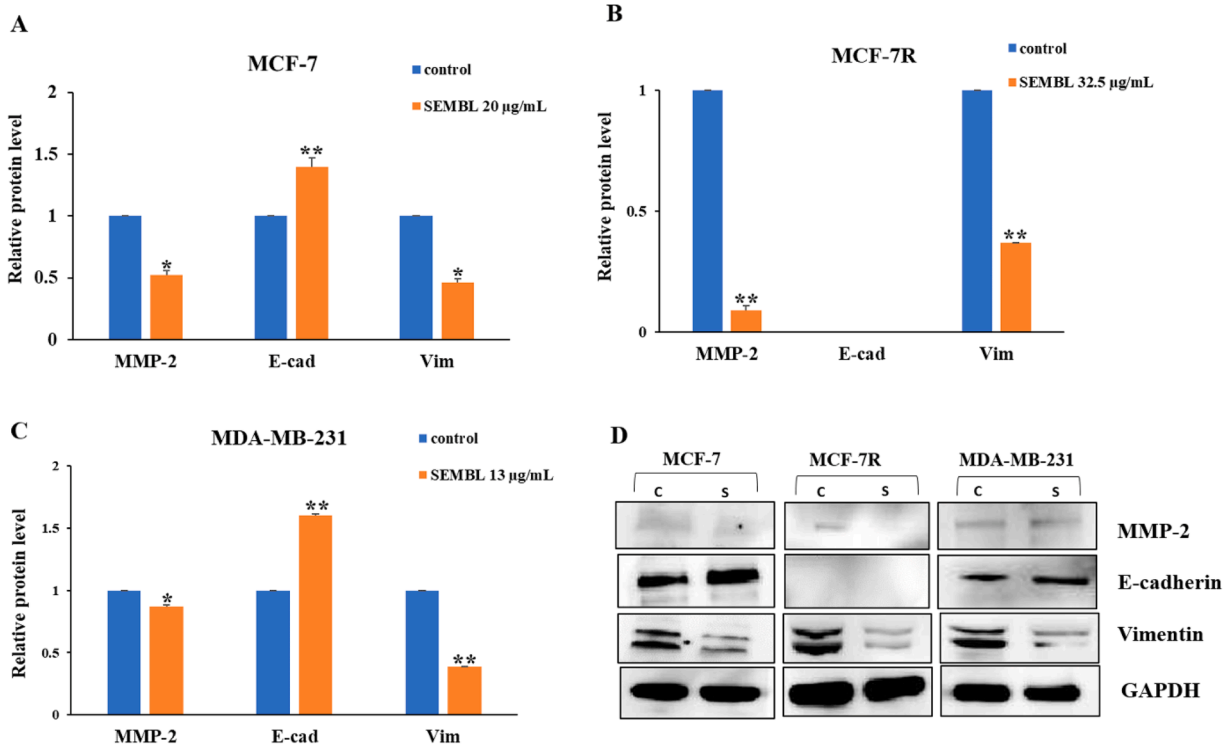

Fig. 9. Western blotting analysis of MMP-2, E-cadherin and Vimentin levels in 3D models. **A.** MCF-7 cells treated for 24 h with SEMBL 20 μg/mL; **B.** MCF-7R cells treated for 24 h with SEMBL 32.5 μg/mL; **C.** MDA-MB-231 cells treated for 24 h with SEMBL 13 μg/mL. The results are expressed as the mean ± standard error of two different experiments. Differences when treatments are compared to control: **p<0.01, *p<0.05 (Tukey's test). **D.** Results of a representative experiments. C: control, S: SEMBL.

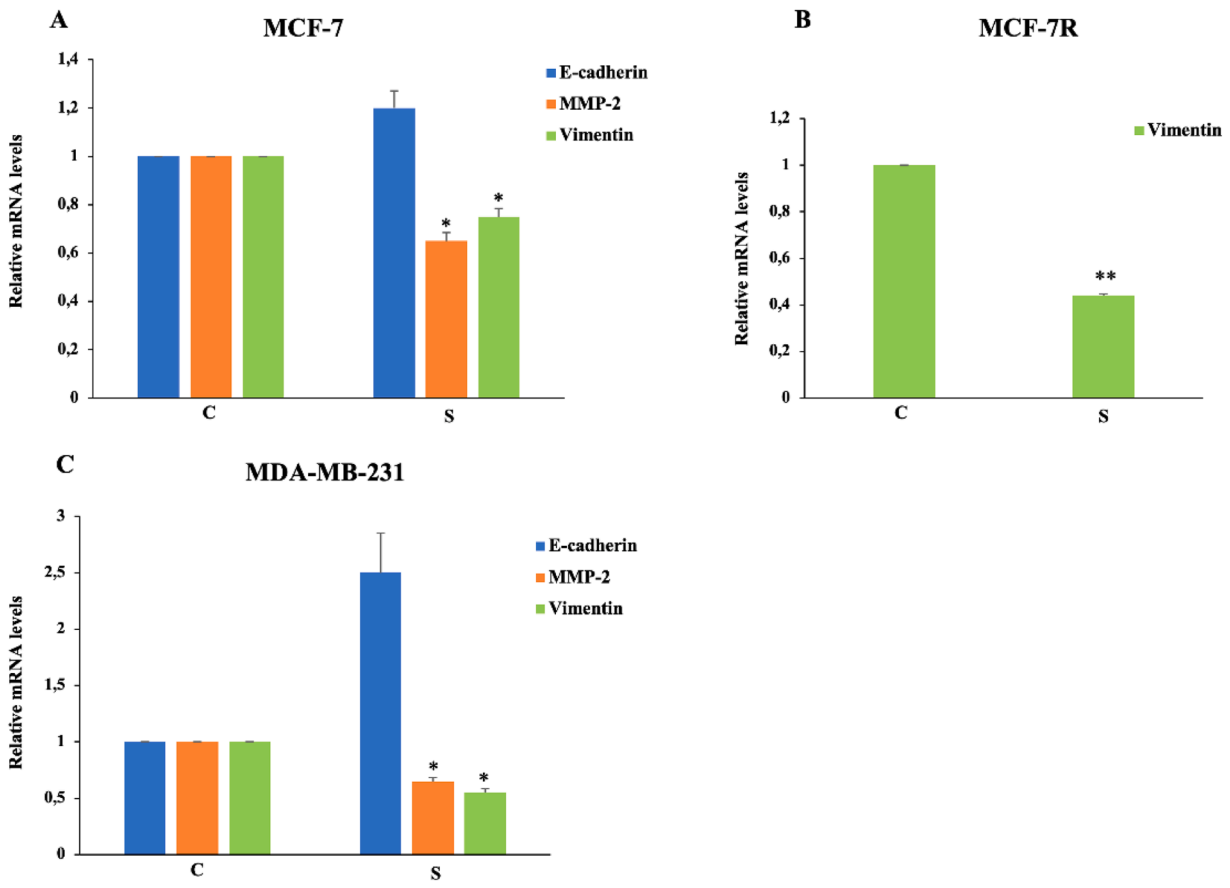

Fig. 11. Evaluation of MMP-2, E-cadherin and Vimentin mRNA expression levels by qRT-PCR in 3D models. For each condition, N=3 technical replicates were used. Data are expressed as mean ± standard error of two experiments. In particular cells were treated as well as for protein expression detection: **A.** MCF-7 cells treated for 24 h with SEMBL 20 μg/mL; **B.** MCF-7R cells treated for 24 h with SEMBL 32.5 μg/mL; **C.** MDA-MB-231 cells treated for 24 h with SEMBL 13 μg/mL. Differences when treatments are compared to control: **p<0.005, *p<0.05 (Tukey's test). C: control, S: SEMBL.

Consent for publication

All authors give consent for the publication of this manuscript.

CRediT authorship contribution statement

Monica Notarbartolo: Writing – review & editing, Supervision, Project administration, Funding acquisition, Conceptualization. **Jun Ma:** Formal analysis, Data curation. **Alessandra Cusimano:** Formal analysis, Data curation. **Francesco Pavia:** Writing – review & editing, Formal analysis, Data curation. **Camilla Carbone:** Formal analysis, Data curation. **Salvatrice Rigogliuso:** Methodology, Formal analysis, Data curation. **Manuela Labbozzetta:** Formal analysis, Data curation. **Paola Poma:** Writing – review & editing, Writing – original draft, Project administration, Formal analysis, Conceptualization.

Declaration of Competing Interest

The authors declare that they have no known competing financial interests or personal relationships that could have appeared to influence the work reported in this paper.

Acknowledgments

The authors gratefully thank Professor Kazuo Umezawa, Dr. Yinzhi Lin, Dr. Keyu Hu and Professor Fabiana Geraci.

Appendix A. Supporting information

Supplementary data associated with this article can be found in the online version at doi:10.1016/j.biopha.2024.117552.

References

[1] Y. Liang, H. Zhang, X. Song, Q. Yang, Metastatic heterogeneity of breast cancer: molecular mechanism and potential therapeutic targets, Semin. Cancer Biol. 60 (2020) 14–27.
[2] M. Salamone, S. Rigogliuso, A. Nicosia, S. Campora, C.M. Bruno, G. Ghersi, 3D collagen hydrogel promotes in vitro langerhans islets vascularization through ad-MVFs angiogenic activity, Biomedicines 9 (2021) 739.
[3] A. Gandalovičová, D. Rosel, M. Fernandes, P. Veselý, P. Heneberg, V. Čermák, et al., Migrastatics—anti-metastatic and anti-invasion drugs: promises and challenges, Trends Cancer 3 (2017) 391–406.
[4] J. Ma, Y. Zhang, T. Sugai, T. Kubota, H. Keino, M. El-Salhy, et al., Inhibition of cellular and animal inflammatory disease models by NF-κB inhibitor DHMEQ, Cells 10 (2021) 2271.
[5] K. Umezawa, A. Breborowicz, S. Gantsev, Anticancer activity of novel NF-B inhibitor DHMEQ by intraperitoneal administration, Oncol. Res. 28 (2020) 541–550.
[6] K. Sidthipong, J. Ma, W.L. Yu, Y.F. Wang, S. Kobayashi, S. Kishino, et al., Rational design, synthesis and in vitro evaluation of novel exo-methylene butyrolactone salicyloylamide as NF-κB inhibitor, Bioorg. Med. Chem. 27 (2017) 562–566.
[7] M.A. Huber, N. Azoitei, B. Baumann, S. Grünert, A. Sommer, H. Pehamberger, et al., NF-κB is essential for epithelial-mesenchymal transition and metastasis in a model of breast cancer progression, J. Clin. Investig. 114 (2004) 569–581.
[8] M. Kapałczyńska, T. Kolenda, W. Przybyła, M. Zajączkowska, A. Teresiak, V. Filas, et al., 2D and 3D cell cultures – a comparison of different types of cancer cell cultures, Aoms (2016).
[9] M.E. Lombardo, F. Carfì Pavia, I. Vitrano, G. Ghersi, V. Brucato, F. Rosei, V. La Carrubba, PLLA scaffolds with controlled architecture as potential microenvironment for in vitro tumor model, Tissue Cell 58 (2019) 33–41.

[10] B.G. Zhou, C.S. Wei, S. Zhang, Z. Zhang, H.M. Gao, Matrine reversed multidrug resistance of breast cancer MCF-7/ADR cells through PI3K/AKT signaling pathway, J. Cell Biochem. 119 (2018) 3885–3891.
[11] P. Poma, M. Notarbartolo, M. Labbozzetta, A. Maurici, V. Carina, A. Alaimo, et al., The antitumor activities of curcumin and of its isoxazole analogue are not affected by multiple gene expression changes in an MDR model of the MCF-7 breast cancer cell line: analysis of the possible molecular basis, Int. J. Mol. Med. (2007).
[12] P. Poma, M. Labbozzetta, N. D'Alessandro, M. Notarbartolo, NF-κB is a potential molecular drug target in triple-negative breast cancers, OMICS A J. Integr. Biol. 21 (2017) 225–231.
[13] K. Umezawa, Y. Lin, Inhibition of matrix metalloproteinase expression and cellular invasion by NF-κB inhibitors of microbial origin, Biochim. Biophys. Acta (BBA) Proteins Proteom. 1868 (2020) 140412.
[14] A.T. Jacobs, D.Martinez Castaneda-Cruz, M.M. Rose, L. Connelly, Targeted therapy for breast cancer: an overview of drug classes and outcomes, Biochem. Pharmacol. 204 (2022) 115209.
[15] S. Loibl, P. Poortmans, M. Morrow, C. Denkert, G. Curigliano, Breast cancer, Lancet 397 (2021) 1750–1769.
[16] T.A. Brown, E.A. Mittendorf, D.F. Hale, J.W. Myers, K.M. Peace, D.O. Jackson, et al., Prospective, randomized, single-blinded, multi-center phase II trial of two HER2 peptide vaccines, GP2 and AE37, in breast cancer patients to prevent recurrence, Breast Cancer Res. Treat. 181 (2020) 391–401.
[17] A.J. Kerr, D. Dodwell, P. McGale, F. Holt, F. Duane, G. Mannu, et al., Adjuvant and neoadjuvant breast cancer treatments: a systematic review of their effects on mortality, Cancer Treat. Rev. 105 (2022) 102375.
[18] The Cancer Genome Atlas Network. Comprehensive molecular portraits of human breast tumours, Nature. 490 (2012) 61–70.
[19] S. Al-Mahmood, J. Sapiezynski, O.B. Garbuzenko, T. Minko, Metastatic and triple-negative breast cancer: challenges and treatment options, Drug Deliv. Transl. Res. 8 (2018) 1483–1507.
[20] G. Arpino, M. Milano, S. De Placido, Features of aggressive breast cancer, Breast 24 (2015) 594–600.
[21] R. Duchnowska, R. Dziadziuszko, B. Czartoryska-Arłukowicz, B. Radecka, B. Szostakiewicz, K. Sosińska-Mielcarek, et al., Risk factors for brain relapse in HER2-positive metastatic breast cancer patients, Breast Cancer Res. Treat. 117 (2009) 297–303.
[22] H. Kennecke, R. Yerushalmi, R. Woods, M.C.U. Cheang, D. Voduc, D.C.H. Speers, et al., Metastatic behavior of breast cancer subtypes, JCO 28 (2010) 3271–3277.
[23] M.D. Hackshaw, H.E. Danysh, M. Henderson, E. Wang, N. Tu, Z. Islam, et al., Prognostic factors of brain metastasis and survival among HER2-positive metastatic breast cancer patients: a systematic literature review, BMC Cancer 21 (2021) 967.
[24] M.A. Huber, N. Kraut, H. Beug, Molecular requirements for epithelial–mesenchymal transition during tumor progression, Curr. Opin. Cell Biol. 17 (2005) 548–558.
[25] C. Jubelin, J. Muñoz-Garcia, L. Griscom, D. Cochonneau, E. Ollivier, M.-F. Heymann, et al., Three-dimensional in vitro culture models in oncology research, Cell Biosci. 12 (2022) 155.
[26] G. Conoscenti, T. Schneider, K. Stoelzel, F. Carfì Pavia, V. Brucato, C. Goegele, et al., PLLA scaffolds produced by thermally induced phase separation (TIPS) allow human chondrocyte growth and extracellular matrix formation dependent on pore size, Mater. Sci. Eng. C. 80 (2017) 449–459.
[27] M.E. Lombardo, G. Zito, F.Carfì Pavia, G. Pizzolanti, C. Giordano, V. Brucato, et al., 3D polymeric supports promote the growth and progression of anaplastic thyroid carcinoma, Biochem. Biophys. Res. Commun. 531 (2020) 223–227.
[28] L.D.C. Stankevicins, M. Urbanska, A.D. Flormann, E. Terriac, Z. Mostajeran, A.K. B. Gad, et al., Vimentin provides the mechanical resilience required for amoeboid migration and protection of the nucleus, Biophysics (2019).
[29] K. Strouhalova, M. Přechová, A. Gandalovičová, J. Brábek, M. Gregor, D. Rosel, Vimentin intermediate filaments as potential target for cancer treatment, Cancers 12 (2020) 184.